

Surface and Tribological Chemistry of Water and Carbon Dioxide on Copper Surfaces

Octavio Furlong · Zhenjun Li · Feng Gao ·
Wilfred T. Tysoe

Received: 29 April 2008 / Accepted: 24 July 2008 / Published online: 1 August 2008
© Springer Science+Business Media, LLC 2008

Abstract The tribological chemistry of carbon dioxide and water vapor is studied on copper surfaces at high pressures, with a view to understand the gas-phase lubrication of copper–copper sliding contacts. The adsorption and film formation properties are studied on vapor-deposited copper films in an ultrahigh vacuum chamber using a quartz crystal microbalance. The nature of the reactively formed film is studied after reaction by *ex situ* X-ray photoelectron spectroscopy (XPS). Carbon dioxide adsorbs reversibly on copper, while water vapor adsorbs both reversibly and irreversibly, where XPS reveals that the irreversibly formed film consists of a mixture of cuprous oxide/hydroxide. Measuring the thickness of the cuprous oxide/hydroxide film as a function of water vapor pressure and temperature reveals that its thickness varies between about 6 and 14 Å and is proportional to the total amount of water adsorbed on the surface. This results in a cuprous oxide/hydroxide film that is thinner at higher temperatures. Measurements of the friction coefficient as a function of temperature and pressure in the presence of water vapor shows that it correlates with film thickness, reaching a limiting value of ~ 0.35 for thicker films.

Keywords Copper · Water vapor · Carbon dioxide · X-ray photoelectron spectroscopy · Quartz crystal microbalance · Friction coefficient · Ultrahigh vacuum tribometer

1 Introduction

Additives are often incorporated into liquid lubricants that react at the tribological interface to form friction- or wear-reducing films. For example, sulfur-containing additives react to form a sulfide, and those containing chlorine form low-friction ferrous chloride layers on iron [1–9], and more complex additives such as zinc dialkyl dithiophosphate have correspondingly more complex surface chemistry, ultimately resulting in the formation of a glassy anti-wear film [10–15]. Such film-forming surface reactions can be thought of as occurring in two steps, the first being the adsorption of the additive onto the surface, followed by a chemical reaction to form the surface film. The temperature dependence of the film-formation reaction therefore depends both on the heat of adsorption, $\Delta H_{\text{(ads)}}$ of the additive and the activation energy E_{act} of the subsequent reaction [16]. In general, the amount of additive that adsorbs on the surfaces (the coverage) will decrease with increasing temperature, while the reaction rate increases with increasing temperature. Thus, the overall rate of film formation, in principle, can either increase or decrease with increasing temperature, depending on the relative magnitudes of the heat of adsorption and the reaction activation energy.

The steady-state thickness of the friction-reducing or anti-wear film arises from a balance between its growth rate and the rate at which it is worn from the surface. Since the wear rate increases with increasing load, and higher normal loads lead to higher interfacial temperatures due to Joule (frictional) heating, lubricant additives should ideally react more rapidly with increasing temperature, and this is generally found to be the case [1–15, 17]. That is, the film growth kinetics of the additive respond to the severity of the tribological conditions. However, in situations in which a current

O. Furlong · Z. Li · F. Gao · W. T. Tysoe (✉)
Department of Chemistry and Biochemistry, and Laboratory for
Surface Studies, University of Wisconsin-Milwaukee,
Milwaukee, WI 53211, USA
e-mail: wtt@uwm.edu

also passes through the tribo-contact, such as in an electrical motor, the situation is less straightforward. To compensate for the increased wear rates at higher loads, the reactive component of the lubricant should react more rapidly at higher temperatures for the reasons outlined above. However, in current-carrying contacts, the interfacial temperature rises not only due to frictional heating, but also due to Ohmic heating because of the current passing through the contact, and thus through the film. The interfacial resistance R increases with increasing film thickness [18, 19], where the power generated is given by i^2R (where i is the constant current and R the resistance of the tribocontact). In this case, if the film were to grow more rapidly at higher temperatures, Ohmic heating would cause the temperature to rise, thus causing the film formation rate to increase to produce a thicker film, thereby producing an even higher temperature due to increased Ohmic heating, and so on. That is, lubricant additives that would be expected to be effective in the absence of a current passing through the interface are likely to produce catastrophic failure when a current passes due to Ohmic heating. Thus, in current-carrying contacts, the tribochemistry should be selected such that the film growth rate *decreases* with increasing temperature to provide a system that is stable with respect to Ohmic heating. However, based on the arguments outlined above, surface chemistry that results in a thinner film at higher temperatures will be inherently unstable with respect to frictional heating. In general, engineering solutions must be sought for current-carrying contacts to address the problem of frictional heating, by ensuring that the system is adequately cooled, or by selecting contacts that are inherently lubricious. Graphite electrical contacts can fulfill the latter requirement since they are electrically conducting and are self-lubricating. However, in very high current applications, the resistance of graphite may still be too high. In addition, any graphite wear debris is also conductive and may produce shorts in the system [18, 19]. One solution to this problem has been to use conductive, metallic copper contacts, since copper has high thermal and electrical conductivities. Indeed these properties are related through the Wiedemann–Franz relationships since they both rely on electron mobility [20]. Since a bare copper–copper contact exhibits high friction, it is necessary, in this case, to lubricate the interface. To be stable with respect to Ohmic heating, as argued above, thinner films should be formed at higher temperatures. In addition, if the contact is required to pass large currents, the resistance of the tribofilm should be as low as possible. In principle, this can be achieved by selecting a chemistry that leads to a film material that conducts electricity well and/or produces a film that is thin. It has been shown previously that complete coverage of surfaces by a monolayer film of an inorganic material is sufficient to reduce the friction coefficient to its minimum value [21–23]. Thus, ideally the surface film

growth kinetics should be self-limiting in the sense that reaction should occur rapidly to form a monolayer film, but slow down substantially once this has been formed. Such film growth behavior has been observed and modeled theoretically by Cabrera and Mott [24]. In this case, a film initially grows rapidly due to the enhanced ion mobility induced by the presence of a large electric field across the film when it is very thin. As the film grows, the electric field decreases causing the film growth rate to decrease.

A mixture of carbon dioxide and water has been used for copper–copper electrical contacts [25–27]. This gas-phase lubricant has the additional advantage of being readily available and environmentally benign. The following explores the surface chemistry of water and carbon dioxide on copper surfaces with the goal of understanding the thermal tribochemistry.

A substantial amount of work has been carried out to study the adsorption of water on transition-metal surfaces [28, 29]. In particular, recent in situ X-ray photoelectron spectroscopy (XPS) measurements reveal that water dissociation is structure sensitive and occurs to form surface hydroxyl species on Cu(110), while the (111) face is completely unreactive [30, 31].

2 Experimental Methods

All experiments were carried out using clean copper surfaces prepared in an ultrahigh vacuum (UHV). Adsorption measurements were made using a quartz crystal microbalance film thickness monitor [32] inserted into a stainless steel, UHV chamber operating at a base pressure of $\sim 1 \times 10^{-9}$ Torr following bakeout. The sample temperature was varied by circulating water through the thickness monitor from an external, thermostatted water bath, where the water temperature was controlled to ± 1 K. Copper was evaporated from a small alumina tube furnace as described elsewhere [33]. A thermocouple was inserted into a copper pellet placed inside the furnace, and it was found that reproducible copper deposition rates could be obtained by controlling the pellet temperature. Experiments were performed by initially depositing 350 Å of copper onto the quartz crystal, then exposing it to various pressures of reactant gases and allowing the system to stabilize for a period of 60 min to make measurements of the mass change and therefore the amount of material adsorbed onto the surface. Following each series of experiments, the vacuum chamber was evacuated, and baked to ~ 100 °C to obtain UHV once again to allow another series of experiments to be performed on a fresh film.

X-ray photoelectron spectra (XPS) were collected in a UHV chamber operating at a base pressure of 2×10^{-10} Torr, as described previously [21–23]. In this

case, experiments were carried out on a clean copper foil that could be resistively heated.

Tribological measurements were made on a copper foil in another stainless steel, UHV chamber operating at a base pressure of $\sim 2 \times 10^{-10}$ Torr following bakeout, which also has been described in detail elsewhere [21–23]. This chamber was equipped with an UHV-compatible tribometer that simultaneously measures normal and lateral forces, as well as the contact resistance between the tip and substrate. All tribological measurements were made using a single pass in the same direction with a sliding speed of 4×10^{-3} m/s with a load of 0.15 N on a freshly prepared surface, and the tribopin was heated by electron bombardment in vacuo prior to each experiment to clean it. Clean copper foil samples were attached to a sample manipulator by mounting them onto a steel plate (0.25 mm thick) to provide a rigid base for the tribological measurements. The tribopin (12.7 mm diameter) was made from tungsten carbide containing some cobalt binder and was cleaned by electron beam heating via a retractable filament that could be placed in front of the pin.

This chamber was equipped with an isolatable reaction cell that could be pressurized with water vapor to form a tribofilm. The sample could then be transferred into the UHV chamber after the cell had been evacuated to carry out friction measurements. Alternatively, the vacuum chamber itself could be pressurized with carbon dioxide and/or water vapor and tribological measurements made in situ.

The copper foil was cleaned by a combination of Argon ion bombardment (~ 2 kV, ~ 2 μ A/cm²) and heating in UHV to ~ 850 K. The sample cleanliness was monitored using Auger and XPS, and the sample was judged to be clean when no signals due to contaminants (primarily carbon and oxygen) were detected. The chamber was then pressurized with water vapor or carbon dioxide for a given period, following which the chamber was evacuated and the XPS recorded. Spectra were typically collected with a Mg K α source power of 250 W and the photoelectrons detected by means of a double-pass, cylindrical-mirror analyzer operating at a pass energy of 50 V.

3 Results

3.1 Carbon Dioxide Adsorption on Copper

The adsorption of carbon dioxide was studied on thin copper films evaporated onto the quartz crystal of the microbalance. Typical results for the mass change per unit area as a function of carbon dioxide pressure, in this case for a sample held at 333 K, are displayed in Fig. 1. Here, the open symbols are for experiments carried out as the carbon dioxide pressure increases, while the filled symbols are the mass changes measured for decreasing pressures.

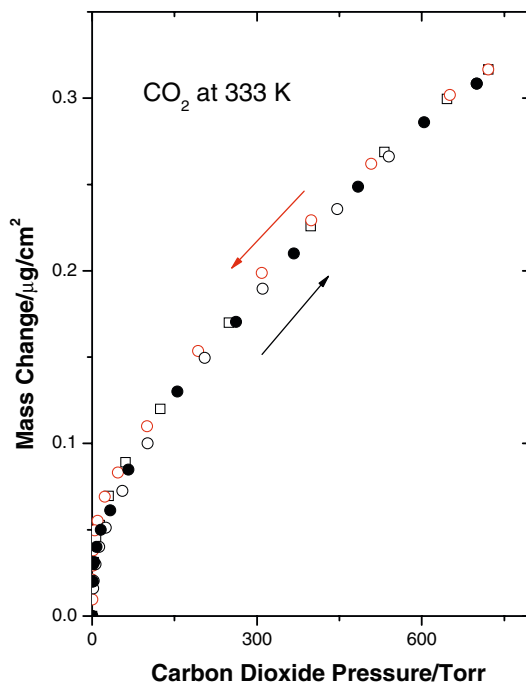


Fig. 1 Adsorption isotherms for carbon dioxide measured on an evaporated copper film using a quartz crystal microbalance at a sample temperature of 333 K measured for increasing pressures (open symbols) and decreasing pressures (filled symbols)

Adsorption is completely reversible indicating that carbon dioxide merely physisorbs on copper without undergoing any reaction with the surface. This result is in accord with previous studies on copper surfaces [34]. For example, a dissociation probability of $\sim 1 \times 10^{-10}$ was found at a temperature of ~ 500 K with an activation energy of ~ 69 kJ/mol. Extrapolating these data to the temperature range relevant to the experiments carried out here (between 293 and 353 K) yields dissociation probabilities of $\sim 1 \times 10^{-13}$ at 353 K to $\sim 1 \times 10^{-15}$ at 293 K. Calculating the collision frequency of carbon dioxide with the surface assuming that it behaves as a perfect gas and assuming a site density of $\sim 1 \times 10^{15}$ /cm² shows that only 8% of the surface would be covered by dissociation products at the highest temperature, 353 K, decreasing to $\sim 0.07\%$ of the surface at 293 K.

The reproducibility of these measurements emphasizes the stability of the quartz crystal microbalance experiments for measuring small mass changes. Measurements of the friction of copper foils exposed to 760 Torr of carbon dioxide showed no significant reduction in friction from that of the clean copper foil (data not shown) in accord with these data.

3.2 Water Vapor Adsorption and Reaction

Figure 2 shows typical isotherms for the adsorption of water vapor on an evaporated copper film collected using

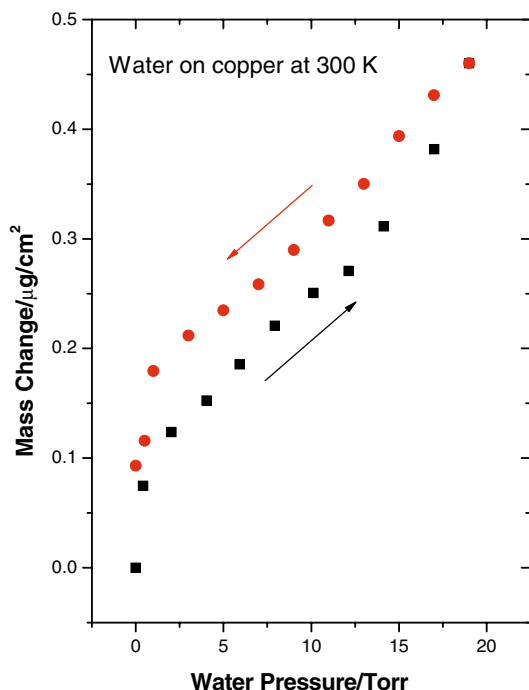


Fig. 2 Adsorption isotherms for water vapor measured on an evaporated copper film using a quartz crystal microbalance at a sample temperature of 300 K for increasing (■) and decreasing pressures (●)

the quartz crystal microbalance, which plots the mass change per unit area as a function of pressure for a sample held at 300 K. Both the mass change with increasing (■) and decreasing (●) pressure are displayed where now, unlike the data for carbon dioxide (Fig. 1), adsorption is not reversible and there is a residual mass change of $\sim 0.1 \mu\text{g}/\text{cm}^2$ after the chamber was evacuated. This indicates that water vapor has reacted with the copper surface to form an irreversibly adsorbed film. This behavior will be discussed in greater detail below.

To establish the nature of this film, XPS were collected for a copper foil that had reacted with 18 Torr of water vapor for 60 min, following which the chamber was evacuated to $\sim 1 \times 10^{-9}$ Torr to collect XPS. Figure 3 displays a typical series of XPS, in this case for a film grown at 300 K, showing the spectra obtained immediately after reaction at 300 K as well as after annealing in vacuo at 393, 513, 643 and, in some cases, 763 K, where the annealing temperatures are marked adjacent to each spectrum. The traces marked background (BG) are spectra for the copper foil prior to reaction with water vapor. Figure 3a displays the Cu 2*p* spectra with a Cu 2*p*_{3/2} feature at 932.6 ± 0.1 eV binding energy (BE) and a 2*p*_{1/2} peak at 952.4 ± 0.1 eV BE. The spin-orbit splitting between the Cu 2*p*_{3/2} and 2*p*_{1/2} features is in good agreement with other data for copper, and the BE does not change with annealing

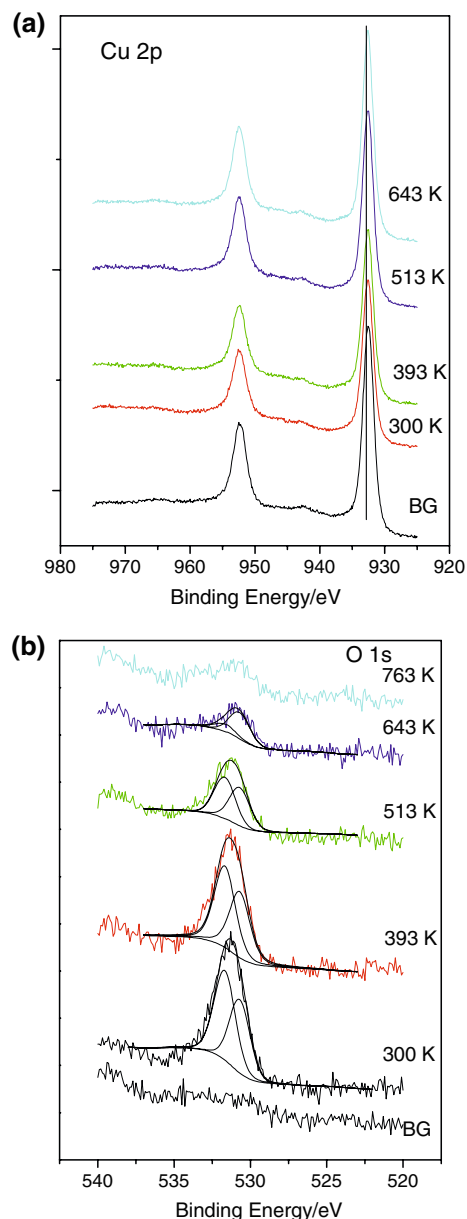


Fig. 3 X-ray photoelectron spectra of a copper foil reacted with 18 Torr of water vapor for 60 min at 300 K showing (a) the Cu 2*p* region and (b) the O 1*s* region. Shown as solid lines in spectra (b) are fits to the O 1*s* profiles

temperature [35]. This BE is consistent with the presence of either Cu(0) or Cu(I) species on the surface, and the BE shift between these copper oxidation states is sufficiently small that they cannot be separated at our resolution [36]. However, these results do allow us to exclude the formation of Cu(II) species since the BE in this case would be ~ 529.5 eV [35]. Surface oxidation is confirmed by the O 1*s* spectral region shown in Fig. 3b. The cleanliness of the sample before reaction is emphasized by the lack of features in the BG spectrum. The spectra display a relatively

broad O 1s feature after reaction at 300 K with 18 Torr of water vapor that decreases in intensity and shifts to 531.4 ± 0.1 eV on heating to 390 K. The profiles at lower temperatures are therefore fit to two Gaussian peaks, one at 531.6 ± 0.2 eV and another at 530.6 ± 0.2 eV. In this case, the BG was removed using the Shirley method [37]. The widths at half height and positions of these features are held constant for all subsequent fits and only the intensity of the components is allowed to vary. This yields good fits to all the data suggesting that this is a reasonable fitting protocol. The feature at ~ 530.6 eV BE is assigned to an oxide species suggesting, based on the observed Cu 2p binding energies, that water reacts with clean copper to form cuprous oxide [30, 31]. The feature at ~ 531.6 eV is assigned to hydroxyl species so that the film comprises a mixed copper oxide/hydroxide [30, 31]. The film is relatively stable on heating to ~ 393 K, and both the oxide and hydroxide features decrease in intensity on heating to ~ 513 K, due to a reduction in the oxide, presumably with the concomitant evolution of water. Further heating to ~ 643 K and above leaves a small amount of surface oxide.

Although the film consists of both oxide and hydroxide components, for simplicity in the following, it will be assumed, for the purposes of estimating the oxide/hydroxide film thickness, that this is comprised entirely of Cu_2O . This copper oxide/hydroxide layer thus provides the friction-reducing film, and its tribological properties will be explored below.

The thickness of the irreversible cuprous oxide/hydroxide film was measured in three ways. In the first, the full adsorption isotherms were collected for water adsorption on an evaporated copper film using a microbalance for various temperatures (as shown in Fig. 2) and reversible water adsorption modeled by a BET isotherm [16], but by including an additional constant-thickness oxide/hydroxide film. This strategy will be described in greater detail below. A second series of experiments were performed in which the evaporated copper film was exposed to various pressures of water vapor at various temperatures for a period of 60 min, the water then evacuated, and the residual mass change measured using the microbalance. Finally, the thickness of the oxide/hydroxide film was estimated from the integrated O 1s intensity measured by XPS compared to that of the Cu 2p feature.

Experiments were carried out to measure the thickness of the cuprous oxide/hydroxide film as a function of water vapor pressure. The results are shown in Fig. 4, where Fig. 4a plots the data for film formation at ~ 300 K and Fig. 4b shows the data collected at ~ 313 K (■). These results were obtained by pressurizing the evaporated copper film with water vapor for 60 min, evacuating the chamber, and then measuring the residual mass change. The x -axis plots the relative water vapor pressure P/P_0 ,

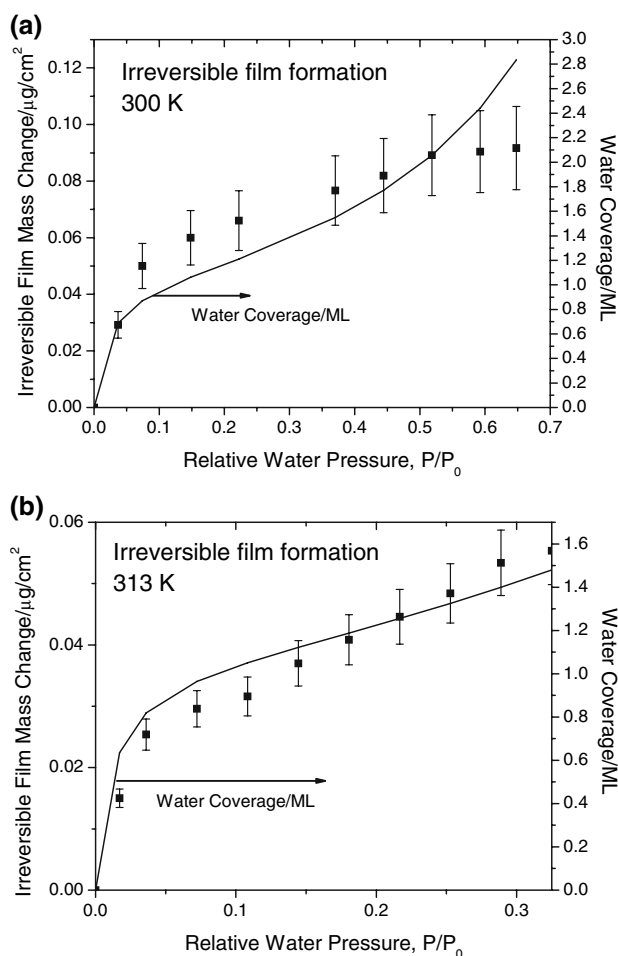


Fig. 4 Plot of the residual mass change due to the formation of an irreversible (cuprous oxide/hydroxide) film measured on an evaporated copper film using a quartz crystal microbalance following reaction at various pressures at (a) 300 and (b) 313 K. Plotted for comparison are the water coverages on the surface (solid lines) calculated from the adsorption isotherm data

where P_0 is the saturated water vapor pressure at the reaction temperature [38]. In both cases (Fig. 4a, b), the mass change due to the formation of the oxide/hydroxide film increases with increasing water vapor pressure, where thicker films are formed at lower temperatures.

The results of similar experiments, where the mass change due to the formation of a copper oxide/hydroxide film using a water vapor pressure of 18 Torr, are plotted as a function of sample temperature in Fig. 5. Results were obtained for an evaporated copper film using the microbalance (●), and reveal that the film thickness decreases with increasing temperature as anticipated from the discussion in the Introduction for a film that must be stable with respect to Ohmic heating. The majority of these data were collected, as described above, using the quartz-crystal microbalance by pressurizing an evaporated copper film with water vapor, evacuating, and then measuring the

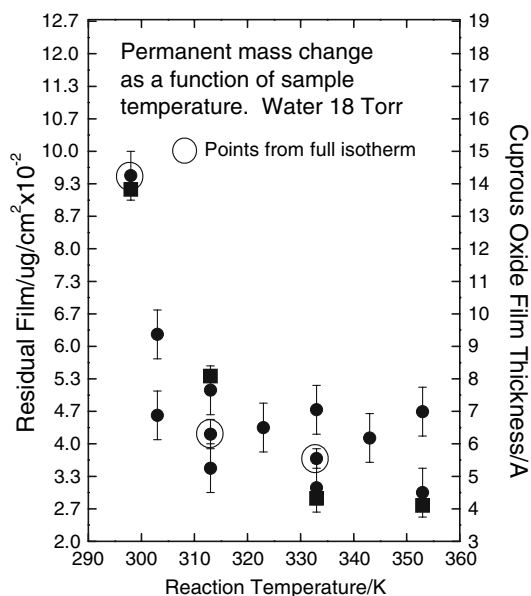


Fig. 5 Plot of the residual mass change due to the formation of an irreversible (cuprous oxide/hydroxide) film measured on an evaporated copper film following reaction at various temperatures measured using a quartz crystal microbalance (●) and by XPS (■). The right hand ordinate shows the corresponding film thickness estimated by assuming that the film consists entirely of cuprous oxide

residual mass change. In some cases, the oxide/hydroxide film thickness was determined using the full isotherm (see below) and the data points for these experiments are circled. Finally, results from XPS measurements on a copper foil (■) are also shown where the data are normalized to a mass change of $9.3 \times 10^{-2} \mu\text{g}/\text{cm}^2$ at 300 K (Fig. 2). These results agree well with those obtained using the quartz crystal microbalance. Plotted on the right ordinate is the estimated film thickness assuming that this consists entirely of cuprous oxide, as a reference.

3.3 Frictional Measurements of Tribofilms Formed from Water on Copper

The frictional properties of copper foils in the presence of water vapor are displayed in Fig. 6, where each measurement was made on a fresh portion of the surface. As a reference, the friction coefficient of the clean copper foil in the absence of water vapor is ~ 1.5 . Figure 6a displays the friction coefficient as a function of water vapor pressure with the sample held at 300 K, showing a monotonic decrease in friction with increasing water vapor pressure to a minimum value of ~ 0.35 , while the data in Fig. 6b shows the effect of increasing temperature in the presence of 18 Torr of water vapor, where the friction coefficient increases with increasing temperature to a maximum value of ~ 0.8 at 353 K.

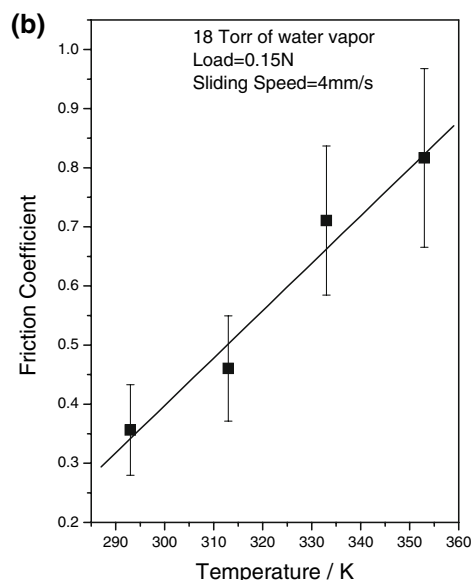
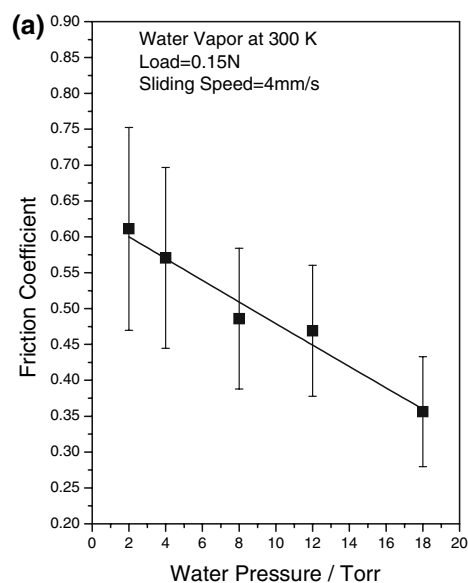


Fig. 6 Plot of the friction coefficient measured in the UHV tribometer for clean copper foils pressurized with water vapor as a function of (a) water vapor pressure at a sample temperature of 300 K and (b) sample temperature at a water vapor pressure of 18 Torr

4 Discussion

The data displayed in Fig. 1 indicate that carbon dioxide alone does not react with copper, as found previously [34]. These results also demonstrate that the microbalance measurements are extremely reproducible and are stable over the relatively long times required to collect the data. This suggests that results for water films should be similarly reproducible. Copper foils exposed to carbon dioxide alone show no substantial decrease in friction coefficient in accord with these data.

The data displayed in Fig. 2 present a typical adsorption isotherm for water adsorbed on copper, in this case at 300 K. The observed hysteresis is interpreted as being due to the formation of an irreversible cuprous oxide/hydroxide film on top of which water adsorbs reversibly. The reversible portion of the data can then be fit to a BET isotherm, which gives the number of adsorbed molecules N_S as

$$\frac{N_S}{B} = \frac{cx}{(1 + (c - 1)x)(1 - x)} \quad (1)$$

where $x = P/P_0$, and P_0 is the saturated vapor pressure at the adsorption temperature T , and B the number of adsorption sites on the surface [16]. This tends to infinity as $x = 1$ due to the formation of a condensed liquid layer. The constant c depends on the heat of adsorption directly on the surface $\Delta H_{(ads)}^S$ and the heat of adsorption in subsequent layers $\Delta H_{(ads)}^L$, where the latter values are taken to be identical for each subsequent adsorption layer and should be close to the heat of vaporization of water. The value of c is given by

$$c = \frac{A \exp(-\Delta H_{(ads)}^S/RT)}{\exp(-\Delta H_{(ads)}^L/RT)} \quad (2)$$

where A is a constant.

The experimental data collected for *decreasing* pressures, where a constant thickness cuprous oxide/hydroxide film is assumed to have formed (Fig. 2), is fit to a BET isotherm (Eq. 1) and the results of the fit are shown in Fig. 7, where a constant film of density $0.095 \pm 0.005 \mu\text{g}/\text{cm}^2$ has been added to the data to account for the presence of the irreversible (oxide/hydroxide) film as indicated by the horizontal dashed line. The resulting mass change is thus the sum of that due to both the (reversible) adsorption of water and the irreversible formation of a cuprous oxide/hydroxide film. The value of $x (=P/P_0)$ was calculated using a saturated vapor pressure of 27 Torr (at 300 K) [38]. Clearly, the fit to the data is good and yields values of $c = 140 \pm 10$. Shown also plotted in Fig. 7 is a line showing the isotherm calculated for adsorption directly onto the surface to form the first monolayer. This indicates that a total of about 3.5 monolayers of water adsorbs on the surface at 300 K at a relative humidity (P/P_0) of 70%. Similar fitting procedures were used for data collected at 313 and 333 K (not shown), and the resulting parameters are summarized in Table 1. Note that since the saturated vapor pressure of water P_0 increases with increasing temperature, the maximum values of x decrease correspondingly for a given water vapor pressure. Thus, while the maximum water coverage at 300 K is almost four monolayers, the maximum water coverage attained at higher temperatures is only slightly larger than a monolayer.

The temperature variation of c is given by Eq. 2 and a plot of $\ln(c)$ versus $1/T$ yields a value for $\Delta H_{(ads)}^L - \Delta H_{(ads)}^S$ and

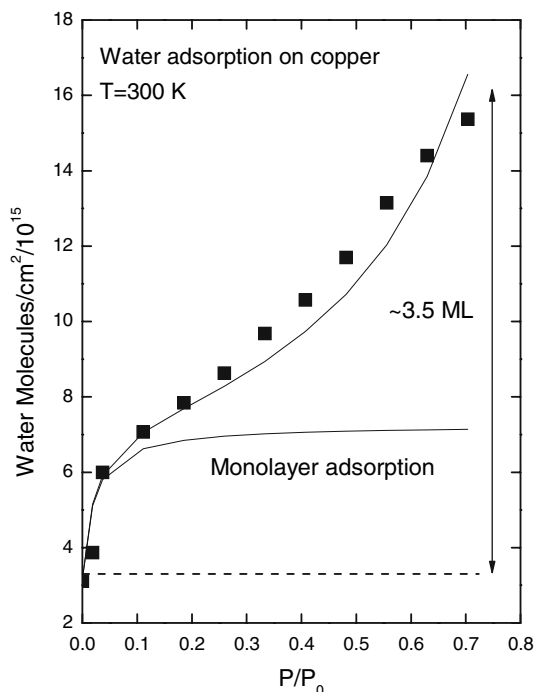


Fig. 7 Typical fit to a water adsorption isotherm showing the mass change due to the formation of an irreversible cuprous oxide/hydroxide film (---) and the coverage of water vapor modeled using a BET isotherm

the data in Table 1 gives $-25 \pm 10 \text{ kJ/mol}$. The heat of vaporization of water (corresponding to $\Delta H_{(ads)}^L$) is $\sim 41 \text{ kJ/mol}$ giving $\Delta H_{(ads)}^S = 65 \pm 10 \text{ kJ/mol}$. The desorption activation energy for water from clean copper varies between ~ 44 and 50 kJ/mol , depending on the surface [39–42]. This is somewhat lower than, but within the ranges of the value from the adsorption isotherm although it should be noted that the adsorption isotherms are for water adsorbed on the cuprous oxide/hydroxide surface rather than on clean copper.

The pressure dependences of the thickness of the films grown at 300 and 313 K are shown in Fig. 4a and b, respectively. These reveal an increase in oxide/hydroxide film thickness with increasing pressure, in both cases. Since copper oxidation occurs by water adsorbing on the surface, it might be expected that just the water adsorbed directly onto the copper oxide/hydroxide surface in the first monolayer in contact with the surface would dictate the extent of oxidation and hence the resulting cuprous oxide/hydroxide film thickness. In fact, the coverage of water directly on the surface (measured as shown in Fig. 7) does not correlate very well with the oxide/hydroxide film thickness. Much better correlation is found with *total* water coverage as indicated by the solid lines plotted in Fig. 4a and b. These plot the total water coverage, measured using

Table 1 Parameters used to fit to adsorption isotherm data for water on copper, where c is the constant defined by Eq. 2, Δm_0 is the mass change due to the cuprous oxide/hydroxide film, and P_0 is the saturated water vapor pressure at the reaction temperature [38]

Temperature/K	c	$\Delta m_0/\mu\text{g}/\text{cm}^2$	P_0/Torr
300	140 ± 10	0.095 ± 0.005	27
313	100 ± 10	0.042 ± 0.002	56
333	50 ± 10	0.037 ± 0.001	150

the quartz crystal microbalance (plotted using the data from Table 1) as a function of P/P_0 and the agreement with the mass change due to the formation of an oxide/hydroxide film is reasonable. This shows that adsorption of the first monolayer results in a mass change due to the oxide/hydroxide film of $4.0 \pm 0.5 \times 10^{-2} \mu\text{g}/\text{cm}^2$, but that the film continues to grow at higher water coverages.

The corresponding temperature dependence of the oxide/hydroxide film thickness at a water vapor pressure of 18 Torr is displayed in Fig. 5, where the results obtained using the microbalance (●) and by XPS (■) are in good agreement. In the latter case, the variation in oxide film thickness on the foil was calculated from the ratio of the integrated intensities of the O 1s to the Cu 2p XPS profiles as a function of reaction temperature. In the case of relatively thick films, the conversion between the intensity ratios and film thickness requires knowledge of the electron escape depth, which control the sampling depth [35]. The films, in this case, are sufficiently thin that these corrections are not necessary, and the film thickness is taken to be approximately proportionate to the intensity ratio.

The data reveal that the oxide/hydroxide film thickness decreases with increasing temperature as anticipated for a tribofilm in an electrical contact. Once again, these data do not correlate well with the first-layer water coverage. However, when the mass change is plotted versus the *total* water coverage in Fig. 8, this reveals a relatively linear correlation between the cuprous oxide/hydroxide film thickness and total water coverage. Note that the decrease in water coverage at higher temperatures arises both from a variation in P/P_0 due to an increase in P_0 with increasing temperature, and from the temperature dependence of c (see Table 1 and Eqs. 1, 2). The results in Fig. 8 again suggest a film thickness that corresponds to a mass change of $(4 \pm 1) \times 10^{-2} \mu\text{g}/\text{cm}^2$ is formed when 1 mL of water is present, in good agreement with the data of Fig. 4, but the films continue to grow as the total water coverage increases.

The film thickness, estimated by assuming that the film consists entirely of cuprous oxide, is plotted on the right ordinate of Fig. 5. This implies that the tribofilm is relatively thin and varies between about 14 \AA at lower temperatures to a limiting value of $6 \pm 2 \text{ \AA}$ as the

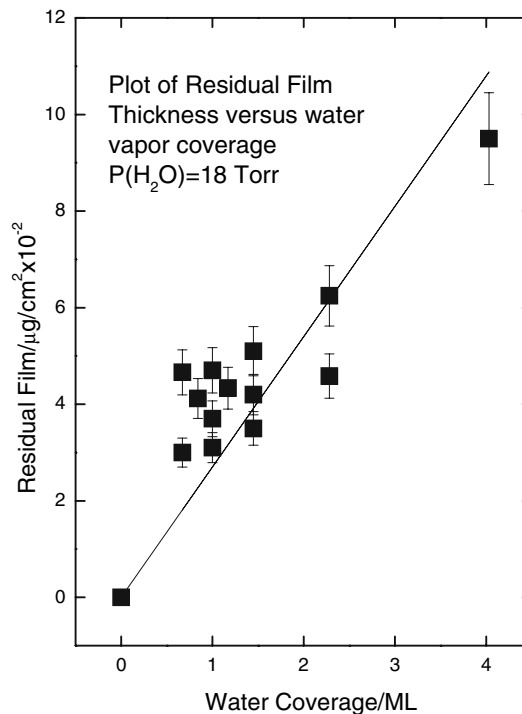


Fig. 8 Plot of the residual mass change due to the reaction of water vapor with a copper film, taken from the data in Fig. 5, versus the water coverage

temperature increases. The lattice spacing of cuprous oxide is 4.26 \AA [43] so that the film thickness at higher temperatures appears to correspond to the formation of approximately a single layer of the oxide. Since this layer also contains hydroxyl species, this is clearly approximate, but does serve to emphasize that reaction with water vapor forms an exceedingly thin layer as would be required for a current-carrying tribofilm.

The friction data displayed in Fig. 6 is in general agreement with the surface chemistry results since both decreasing the water vapor pressure (Fig. 6a) and increasing the temperature (Fig. 6b) result in an increase in friction coefficient corresponding to less adsorbed water, and so producing a thinner cuprous oxide/hydroxide film on the surface. For reference, the friction coefficient of clean copper is ~ 1.5 , and the minimum value of ~ 0.35 is in reasonable agreement with values found previously for cuprous oxide films [36]. The data in Fig. 5 suggest that the film remains reasonably constant in thickness between ~ 210 and 350 K , while the friction coefficient increases over this temperature range. This result suggests that adsorbed water or surface hydroxyl species formed by reaction of the thin oxide film with water vapor may also help reduce friction.

We do note that an asymmetry in the wear of the copper–copper interface has been found depending on the polarity of the current [44, 45]. This asymmetry cannot

arise from the tribochemistry discussed above, since these only incorporate thermal effects, which must be the same for both surfaces. This effect has been explained as being due to a modification of the electric field across the growing film that facilitates ion diffusion, which is either enhanced or diminished depending on polarity to produce an asymmetry [45]. However, a water film may also be present in the tribocontact so that electrochemical effects can also occur. An understanding of film growth in the absence of an external field will provide a baseline for exploring such effects.

5 Conclusions

While carbon dioxide adsorbs reversibly on copper, water vapor reacts with clean copper to form a cuprous oxide/hydroxide film. It is found that the thickness of this irreversibly adsorbed film varies approximately linearly with the total amount of water adsorbed on the surface. Thus, the thickness of the cuprous oxide/hydroxide film increases with increasing water vapor pressure, but decreases with increasing temperature. The variation in friction coefficient as a function of water vapor pressure and temperature is in complete accord with these observations. Since the thickness of the cuprous oxide/hydroxide films depends on the amount of water vapor adsorbed on the surface, the formation of the tribofilm depends on the adsorption of water vapor on top of it rather than the rate at which the water vapor oxidizes the surface. Since both the relative water vapor pressure (P/P_0) and the extent of adsorption decrease with increasing temperature, this behavior gives rise to a thinner film at higher temperatures, as required for a current-carrying tribo-interface. This, however, will lead to an interface that is unstable with respect to frictional heating.

Acknowledgment We gratefully acknowledge the support of this work by the Office of Naval Research.

References

- Kotvis, P.V.: Overview of the chemistry of extreme-pressure additives. *Lubr. Eng.* **42**, 363 (1986)
- Dorinson, A., Ludema, K.C.: *Mechanics and Chemistry in Lubrication*. Elsevier, Amsterdam (1985)
- Lara, J., Surerus, K., Kotvis, P.V., Contreras, M.E., Rico, J.L., Tysoe, W.T.: The surface and tribological chemistry of carbon disulfide as an extreme-pressure additive. *Wear* **239**, 77 (2000). doi:10.1016/S0043-1648(99)00368-3
- Kaltchev, M., Kotvis, P.V., Lara, J., Blunt, T.J., Tysoe, W.T.: A molecular beam study of the tribological chemistry of dialkyl disulfides. *Tribol Lett* **10**, 45 (2001). doi:10.1023/A:1009020725936
- Gao, F., Kotvis, P.V., Tysoe, W.T.: Surface and tribological chemistry of chlorine- and sulfur-containing lubricant additives. *Trib. Int.* **37**, 87 (2004). doi:10.1016/S0301-679X(03)00040-9
- Gao, F., Furlong, O., Kotvis, P.V., Tysoe, W.T.: Reaction of tributyl phosphite with oxidized iron: surface and tribological chemistry. *Langmuir* **20**, 7557 (2004). doi:10.1021/la049438t
- Gao, F., Kotvis, P.V., Stacchiola, D., Tysoe, W.T.: Reaction of tributyl phosphate with oxidized iron: surface chemistry and tribological significance. *Tribol. Lett.* **18**, 375 (2005). doi:10.1007/s11249-004-2768-1
- Gao, F., Furlong, O., Kotvis, P.V., Tysoe, W.T.: Tribological properties of films formed by the reaction of carbon tetrachloride with iron. *Tribol. Lett.* **20**, 171 (2005). doi:10.1007/s11249-005-8313-z
- Furlong, O., Gao, F., Kotvis, P.V., Tysoe, W.T.: Understanding the tribological chemistry of chlorine-, sulfur- and phosphorus-containing additives. *Trib. Int.* **40**, 699 (2007). doi:10.1016/j.triboint.2006.05.011
- Yamaguchi, E.S., Zhang, Z., Kasrai, M., Bancroft, G.M.: Study of the interaction of ZDDP and dispersants using X-ray absorption near edge structure spectroscopy-Part 2. *Tribol. Lett.* **15**, 385 (2003). doi:10.1023/B:TRIL.0000003062.91646.8f
- Nicholls, M.A., Do, T., Norton, P.R., Bancroft, G.M., Kasrai, M., Capelhart, T.W., et al.: Chemical and mechanical properties of ZDDP antiwear films on steel and thermal spray coatings studied by XANES spectroscopy and nanoindentation techniques. *Tribol. Lett.* **15**, 241 (2003). doi:10.1023/A:1024813203442
- Varlot, K., Kasrai, M., Martin, J.M., Vacher, B., Bancroft, G.M., Yamaguchi, E.S., et al.: Antiwear film formation of neutral and basic ZDDP: influence of the reaction temperature and of the concentration. *Tribol. Lett.* **8**, 9 (2000). doi:10.1023/A:1019162529554
- Suominen Fuller, M.L., Rodriguez Fernandez, L., Massoumi, G.R., Lennard, W.N., Kasrai, M., Bancroft, G.M.: The use of X-ray absorption spectroscopy for monitoring the thickness of antiwear films from ZDDP. *Tribol. Lett.* **8**, 187 (2000). doi:10.1023/A:1019195404055
- Bancroft, G.M., Kasrai, M., Fuller, M., Yin, Z., Fyfe, K., Tan, K.H.: Mechanisms of tribochemical film formation stability of tribo- and thermally-generated ZDDP films. *Tribol. Lett.* **3**, 47 (1997). doi:10.1023/A:1019179610589
- Pauli, M.D., Rufael, T.S., Mowlem, J.K., Weinert, M., Saldin, D.K., Tysoe, W.T.: X-ray absorption near-edge structure analysis of the chemical environment of zinc in the tribological films formed by zinc dialkyl dithiophosphate decomposition on steel. *Trib. Int.* **38**, 195 (2005). doi:10.1016/j.triboint.2004.08.007
- Clark, A.: *The Theory of Adsorption and Catalysis*. Academic Press, New York (1970)
- Najman, M.N., Kasrai, M., Bancroft, G.M., Miller, A.: Study of the chemistry of films generated from phosphate ester additives on 52100 steel using X-ray absorption spectroscopy. *Tribol. Lett.* **13**, 209 (2002). doi:10.1023/A:1020164127000
- Slade, P.G.: *Electrical Contacts: Principles and Applications*. Marcel Dekker, New York (1999)
- Holm, R.: *Electrical Contacts: Theory and Applications*. Springer-Verlag, Berlin (1976)
- Kittel, C.: *Introduction to Solid State Physics*. Wiley, New York (1996)
- Wu, G., Gao, F., Kaltchev, M., Gutow, J., Mowlem, J., Schramm, W.C., et al.: An investigation of the tribological properties of thin KCl films on iron in ultrahigh vacuum: modeling the extreme-pressure lubricating interface. *Wear* **252**, 595 (2002). doi:10.1016/S0043-1648(02)00009-1
- Gao, F., Kaltchev, M., Kotvis, P.V., Tysoe, W.T.: The tribological properties of monolayer KCl films on iron in ultrahigh vacuum: modeling the extreme-pressure lubricating interface. *Tribol. Lett.* **14**, 99 (2003). doi:10.1023/A:1021752203606
- Gao, F., Kotvis, P.V., Tysoe, W.T.: The frictional properties of thin inorganic halide films on iron measured in ultrahigh vacuum. *Tribol. Lett.* **15**, 327 (2003). doi:10.1023/A:1024833807985

24. Cabrera, N., Mott, N.F.: Theory of oxidation of metals. Rep. Prog. Phys. **12**, 163 (1949). doi:[10.1088/0034-4885/12/1/308](https://doi.org/10.1088/0034-4885/12/1/308)
25. Gao, C., Kuhlmann-Wilsdorf, D.: Adsorption films, humidity, stick-slip and resistance of sliding contacts. IEEE Trans. Comp. Hybrids Manuf. Tech. **14**, 37 (1991). doi:[10.1109/33.76508](https://doi.org/10.1109/33.76508)
26. Gao, C., Kuhlmann-Wilsdorf, D.: On the tribological behavior of adsorbed layers, especially moisture. Wear **149**, 297 (1991). doi:[10.1016/0043-1648\(91\)90381-4](https://doi.org/10.1016/0043-1648(91)90381-4)
27. Gao, C., Kuhlmann-Wilsdorf, D.: Moisture effects including stiction resulting from adsorbed water films. Trans. ASME J. Trib. **114**, 174 (1992). doi:[10.1115/1.2920857](https://doi.org/10.1115/1.2920857)
28. Henderson, M.A.: The interaction of water with solid surfaces: fundamental aspects revisited. Surf. Sci. Rep. **46**, 1 (2002). doi:[10.1016/S0167-5729\(01\)00020-6](https://doi.org/10.1016/S0167-5729(01)00020-6)
29. Thiel, P.A., Madey, T.E.: The interaction of water with solid surfaces: fundamental aspects. Surf. Sci. Rep. **7**, 211 (1987). doi:[10.1016/0167-5729\(87\)90001-X](https://doi.org/10.1016/0167-5729(87)90001-X)
30. Yamamoto, S., Andersson, K., Bluhm, H., Ketteler, G., Starr, D.E., Schiros, T., et al.: Hydroxyl-induced wetting of metals by water at near-ambient conditions. J. Phys. Chem. C **111**, 7848 (2007). doi:[10.1021/jp0731654](https://doi.org/10.1021/jp0731654)
31. Andersson, K., Ketteler, G., Bluhm, H., Yamamoto, S., Ogasawara, H., Pettersson, L.G., et al.: Bridging the pressure gap in water and hydroxyl chemistry on metal surfaces: the Cu(110) case. J. Phys. Chem. C **111**, 14493 (2007). doi:[10.1021/jp073681u](https://doi.org/10.1021/jp073681u)
32. Steinem, C., Janshoff, A.: Piezoelectric Sensors. Springer, New York (2007)
33. Wytenburg, W.J., Lambert, R.M.: Long-lived aluminum evaporation source for controlled, reproducible deposition of clean ultra-thin films under ultrahigh vacuum conditions. J. Vac. Sci. Technol. **10**, 3579 (1992). doi:[10.1116/1.577787](https://doi.org/10.1116/1.577787)
34. Nakamura, J., Rodriguez, J.A., Campbell, C.T.: Does CO₂ dissociatively adsorb on Cu surfaces? J. Phys. Condens. Matter **1**, SB149 (1989). doi:[10.1088/0953-8984/1/SB/026](https://doi.org/10.1088/0953-8984/1/SB/026)
35. Briggs, D.: Handbook of X-ray and Ultraviolet Photoelectron Spectroscopy. Heyden, London (1977)
36. Rabinowicz, E., Narayan, S.B.: Thickness effects using cupric oxide as a solid lubricant for copper. ASLE Proc. 3rd Int. Conf. Solid Lubrication, 30 (1984)
37. Shirley, D.A.: High-resolution X-ray photoemission spectrum of the valence bands of gold. Phys. Rev. B **5**, 4709 (1972). doi:[10.1103/PhysRevB.5.4709](https://doi.org/10.1103/PhysRevB.5.4709)
38. Gubkov, A.N., Fermor, N.A., Smirnov, N.I.: Vapor pressure of mono-poly systems. Zh. Prikl. Khim. Leningrad **37**, 2204 (1964)
39. Bange, K., Grider, D.E., Madey, T.E., Sass, J.K.: The surface chemistry of H₂O on clean and oxygen-covered Cu(110). Surf. Sci. **137**, 38 (1984). doi:[10.1016/0039-6028\(84\)90675-7](https://doi.org/10.1016/0039-6028(84)90675-7)
40. Lackey, D., Schott, J., Straehler, B., Sass, J.K.: Water adsorption on clean and caesium covered Cu{110}. J. Chem. Phys. **91**, 1365 (1989). doi:[10.1063/1.457160](https://doi.org/10.1063/1.457160)
41. Au, C., Breza, J., Roberts, M.W.: Hydroxylation and dehydroxylation at Cu(111) surfaces. Chem. Phys. Lett. **66**, 340 (1979). doi:[10.1016/0009-2614\(79\)85030-7](https://doi.org/10.1016/0009-2614(79)85030-7)
42. Ovesen, C.V., Stoltze, P., Nørskov, J.K., Campbell, C.T.: A kinetic model of the water gas shift reaction. J. Catal. **134**, 445 (1992). doi:[10.1016/0021-9517\(92\)90334-E](https://doi.org/10.1016/0021-9517(92)90334-E)
43. Wyckoff, R.W.G.: Crystal Structures. Wiley, New York (1963)
44. Belyi, V.A., Konchits, V.V., Savkin, V.G.: Polar effects within the sliding contact of metal-containing brushes. Wear **78**, 249 (1982). doi:[10.1016/0043-1648\(82\)90036-9](https://doi.org/10.1016/0043-1648(82)90036-9)
45. Boyer, L., Noel, S., Chabriere, J.P.: Electrochemically activated wear of metal fibre brushes. Wear **116**, 43 (1987). doi:[10.1016/0043-1648\(87\)90266-3](https://doi.org/10.1016/0043-1648(87)90266-3)